

Application of Remote Sensing Techniques in Enhancement, Detection, and Slicing of Koopan Lateralized Ultrabasics (South of Bavanat, Fars Province)

M. Zurmand¹, A. Ahmadi Khalaji^{1*}, K. Noori Khankahdani², Z. Tahmasbi¹

¹ Department of Geology, Faculty of Sciences, Lorestan University, Khorramabad, Islamic Republic of Iran

² Department of Geology, Shiraz Branch, Islamic Azad University, Shiraz, Islamic Republic of Iran

Received: 6 February 2022 / Revised: 9 November 2022 / Accepted: 3 December 2022

Abstract

Lateritized ultrabasic units are located in the south of Bavanat in the northeast of Fars province in the east of Koopan village. The current study has used Landsat 8 images for RS processing. This study indicated that the RGB=532 color composite in Landsat 8 image has the best contrast for enhancing and detecting peridotite and serpentinite units. Also, based on the band ratio technique, RGB=(b2/b1), (b5/b1), and (b6/b7) color composite has the best contrast for peridotite and serpentinite units. The Principal Component Analysis technique with the standard method followed the best difference to detect and identify the ultrabasics. Principal Component Analysis method shows that RGB=PC6, PC2, and PC5 for Landsat 8 data have the best contrast for enhancement and detection of peridotite and serpentinite units. Finally, different methods of supervised classification, such as Spectral Angle Mapper, Spectral Information Divergence, and Support Vector Machine, were reviewed. Among these methods, the Spectral Information Divergence technique has the best layout for Landsat 8 images. This important layout as a basic geological map can be useful in additional exploration studies on the Bavanat peridotites.

Keywords: Lateritized ultrabasic; Koopan; Principal Component Analysis; Supervised classification, high Zagros.

Introduction

Lateritized ultrabasics result from weathering of ultrabasic rocks in hot and humid climates. Regarding stratigraphy, Koopan laterites are located on Neyriz ophiolites, which are part of the Late Cretaceous Zagros ophiolite series. These laterites are covered with

nomolitic limestones equivalent to Jahrom Formation with Eocene age. So the time of the lateritization event should be after Late Cretaceous and before Eocene, in which case the Paleocene time can be assumed for this event. Lithologically, the study area includes serpentinitized peridotites, red laterites, Eocene limestones, and Quaternary sediments [1]. In order to separate different areas or rock units, in remote sensing,

* Corresponding author: Tel: +989163614569; Email: ahmadikhalaj.a@lu.ac.ir

it is possible to reduce or increase the reflective spectrum of the selected area by using different spectral ratios [2]. The purpose of this technique is that the integration of remote sensing data and field information can spend less time and costs and also use more accurate digital methods, operations enhancement, detection, and slicing of different units to carry out (e.g., Alavipanah [3], Gupta [4], Taherzadeh et al. [5], Sekhavati et al. [6] and Faridi et al. [7]). Gomez et al. [8], using data from Aster satellites, separated ten types of limestone and alluvial sandstone. Nikolakopoulos et al. [9], using data from Landsat satellites, created the geological map of Halki Island, Greece, which depicts the geotectonic units, geological formations, and tectonic structures. Remote sensing is particularly important in geological studies so that this technology can extract valuable information about the studies, including linear structures, identify alteration zones, geomorphological phenomena, etc. [10]. Charou et al. [11] evaluated the utilization of

Landsat, SPOT, and ASTER data for environmental mapping on a local scale. Ruisi et al. [12] used satellite imagery to interpret central Tibet's (China) geological structure. Several researchers have used Remote Sensing techniques to detect and explore mineral resources (e.g., Noori Khankahdani and Zarei [13], Shahvaran et al. [14], Khademi et al. [15], Ghasemi et al. [16]).

In the current research, it has been tried to use field data and remote sensing techniques to identify and strengthen peridotite and serpentinite units in the Kooapan region.

Geological setting

Late Cretaceous Neyriz Ophiolite, as part of the outer Zagros Ophiolitic Belt, is a remnant of the Southern Neo-Tethyan oceanic lithosphere, which is located along the Zagros suture zone in the south of Iran (Figure 1).

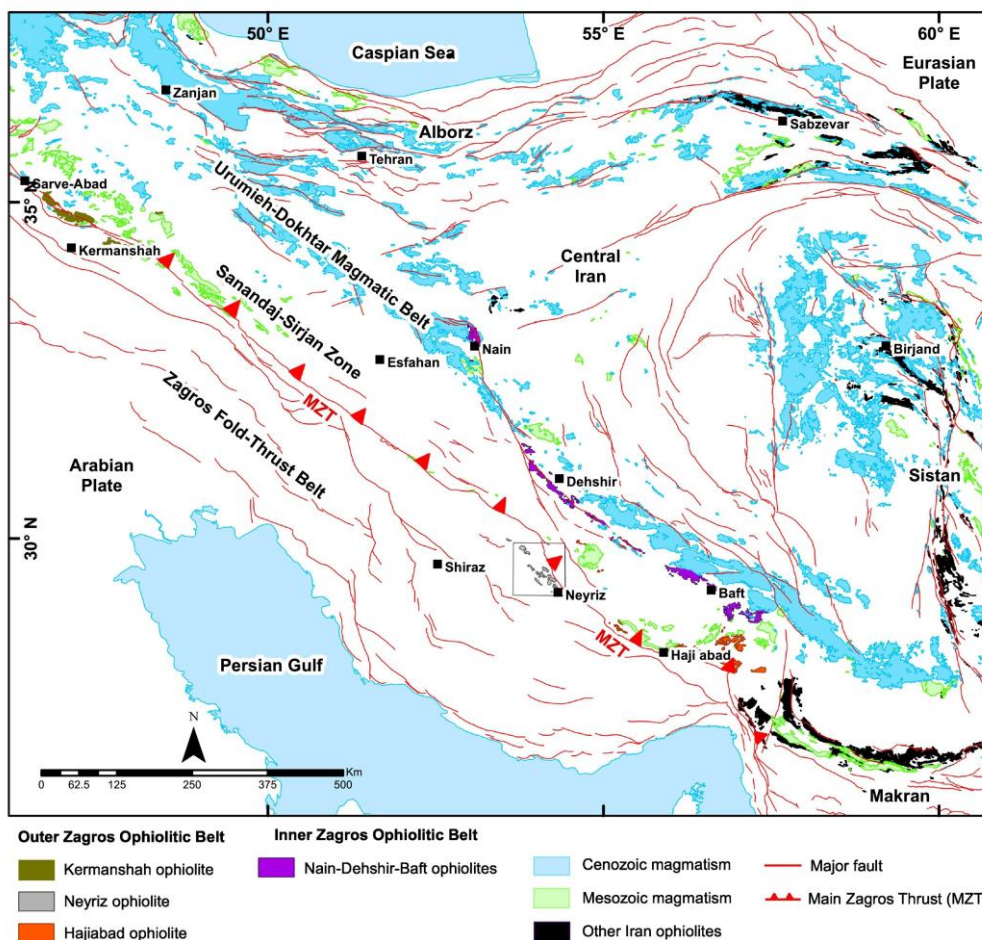


Figure 1. The distribution of the Zagros ophiolites between the boundaries of the Sanandaj-Sirjan Zone with the Zagros Fold-Thrust Belt in the south west (SW) and the Urumieh-Dokhtar Magmatic Belt [17]. The location of the Neyriz ophiolite show in the box.

Regarding the division of structural states, the study area is located in the high Zagros. Neyriz ophiolite formed from the Neo-Tethyan intra-oceanic subduction system, and preserves evidence of the evolution from an early-MORB oceanic crust to an extending fore-arc basin during subduction rollback processes [17]. Neyriz ophiolite consists of three main lithological units including mantle peridotite, intrusive rocks and extrusions. Harzburgites are the dominant peridotites. Intrusive rocks are including accumulations of peridotite, layered gabbros, isotropic gabbros and plagiogranite.

After peridotite, gabbro is the second largest igneous component of the Neyriz ophiolite [18, 19]. The U-Pb zircon geochronology for plagiogranite and gabbro in this ophiolite shows the formation age of 100.1 ± 2.3 to 93.4 ± 1.3 Ma, respectively [17]. Volcanic rocks are mainly including basaltic to andesitic pillow lavas and sheet flows.

Lateritized ultrabasic units are marked marl on geological maps [20]. However, recent studies have shown that these rocks are lateritized ultrabasic rocks [14, 21] (Figure 2). A view of peridotite and

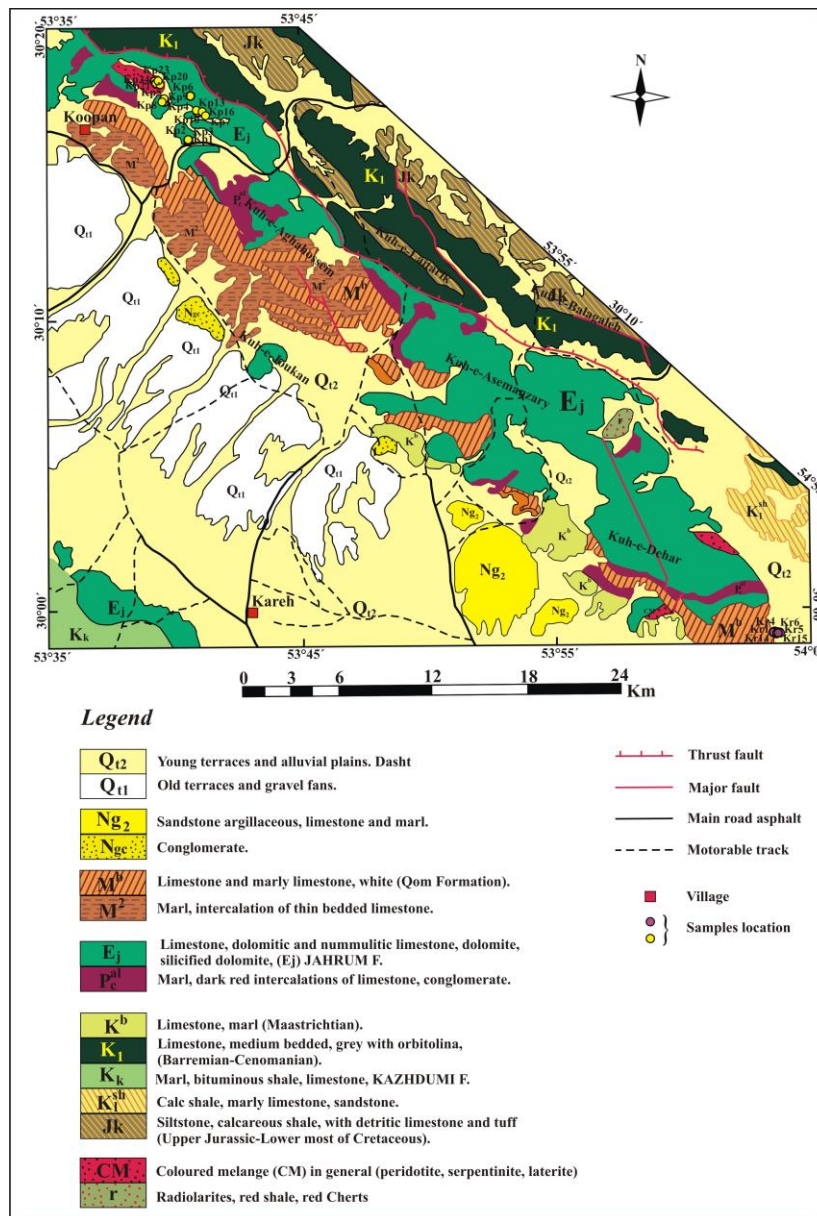


Figure 2. Simplified geological map of the Koopan area (after geological map of Eghlid [20]).

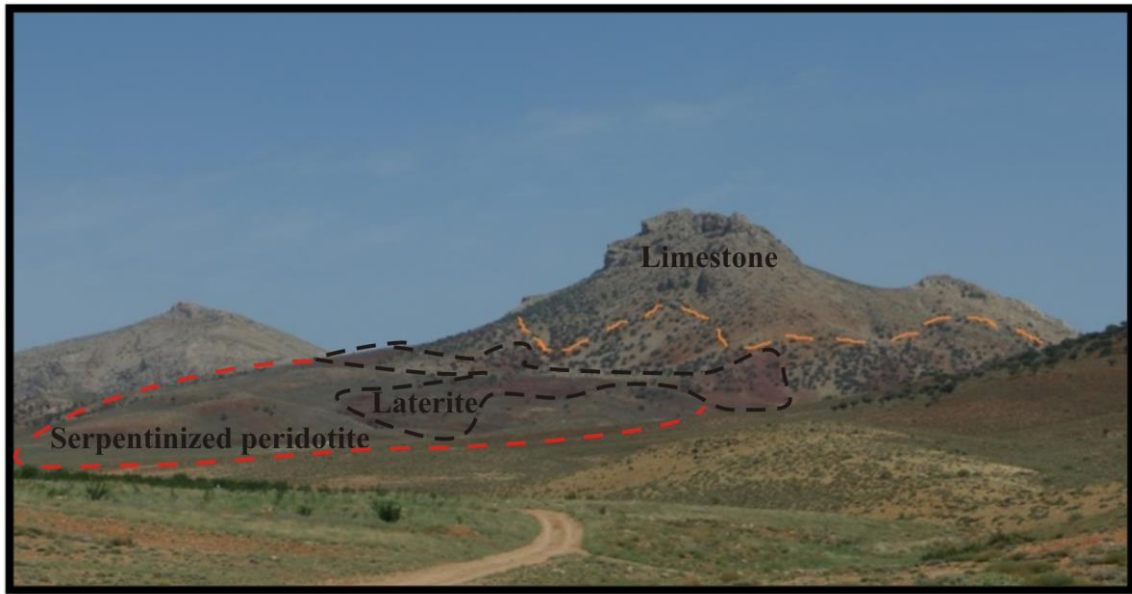


Figure 3. A view of the lateritized ultrabasic units in the Koopan area.



Figure 4. Macroscopic scale of peridotite units in the Koopan area.

serpentinized peridotite units of the koopan region can be seen in Figures 3, 4, and 5. The oldest rock units, including Late Cretaceous ultramafic to mafic rocks (Neo-Tethys oceanic crust), are covered by progressive Paleocene sediments.

Materials and Methods

In this research, outcrops of peridotite and serpentinite were studied. Table 1 shows the geographical coordinates of the peridotite, serpentinite,

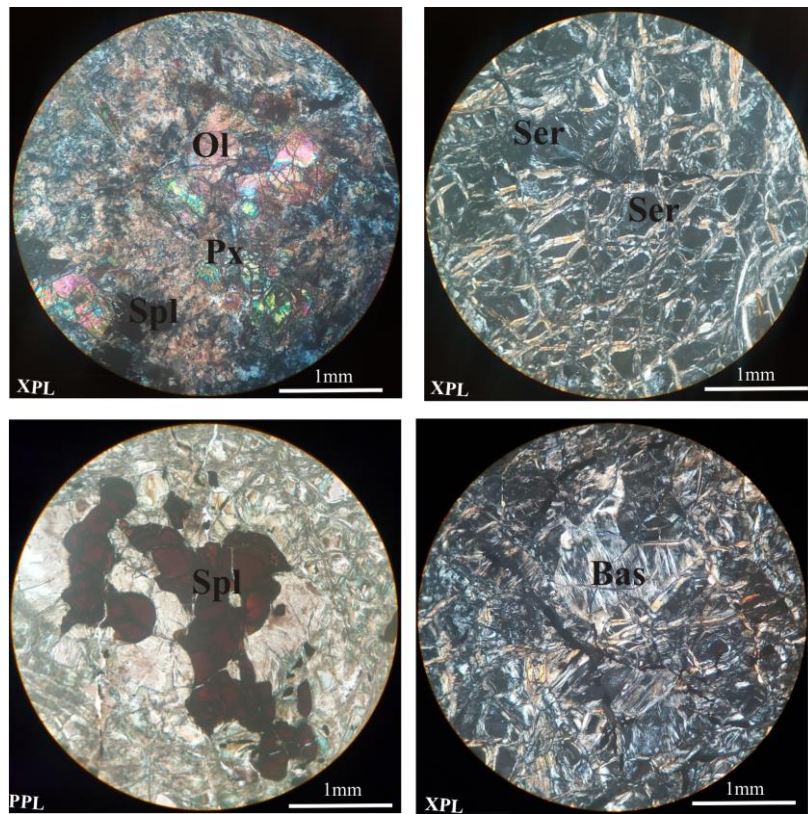


Figure 5. Microscopic photos from serpentinized peridotites of the Neyriz ophiolite in the Koopan area. a) olivine, pyroxene, and serpentine, with a small amount of Cr-spinel in harzburgites, b) Serpentine group minerals in highly serpentinized harzburgites (serpentinite), c) amoeboid chromian spinel in serpentinized harzburgite, d) Orthopyroxene in highly serpentinized harzburgite altered to bastite. Abbreviations: Ol – olivine, Px –pyroxene, Spl – chromian spinel, Serp – serpentine

limestone, and laterite rocks. Thirteen rock samples from peridotites with varying degrees of serpentinization were collected. The sections gathered from serpentinized peridotite rock-types. They were studied by optical microscope. Thin sections of serpentinized peridotites were studied, achieving more information about the mineralogical characteristics of the Koopan area. After field observation and preliminary identification of peridotite and serpentinite samples by microscopic studies, Landsat 8 images were utilized for remote sensing operations. For this purpose, ENVI 5.3 software was used. After pre-processing of data, different methods of remote sensing, such as the construction of color composites, data fusion, band ratio, PCA, and supervised classification, were used. So, peridotite and serpentinite units were detected and separated very well. The results of each section are presented as follows.

Petrography

We collected peridotite samples from Neyriz ophiolite in the Koopan area. The peridotites underwent

varying degrees of serpentinization (Figure 5). Serpentinized peridotite is the most abundant ultramafic rock in Koopan area. Serpentinized harzburgite observes in the most part of the area and occasionally accompanied with small dunite lenses. The harzburgite has a granular texture, with high serpentinization (Fig. 5a). It is consisting mainly of olivine, orthopyroxene, clinopyroxene, serpentine, and Cr-spinel (Fig. 5a). The olivine has varying degrees of serpentinization. Increasing degree of alteration is expressed by growth of secondary minerals (serpentine group). Serpentine group minerals are abundant in harzburgites (Fig. 5b). The spinel has an amorphous or molten shape (Fig. 5c). The pyroxenes show deformational features such as kinking structure. Orthopyroxene in highly serpentinized harzburgite altered to bastite (Fig. 5d). Dunites are seen as lenses within harzburgites. Dunites consist of olivine, pyroxene and Cr-spinel. The olivine and pyroxenes are variably serpentinized into lizardite (dominant) and antigorite.

Table 1. The geographical coordinates of peridotite and serpentinite.

Row	Sample Number	Y	X	Description
1	kp2	30 16 09.5	53 40 33.8	Paleocene limestone
2	kp3	30 16 9.6	53 40 33.5	Paleocene limestone
3	kp4	30 17 34.9	53 39 36.5	limestone
5	kp5	30 17 33.5	53 39 37.2	limestone
6	Kp11	30 17 42	53 40 39	Laterite
7	Kp13	30 17 9.1	53 40 54.5	Laterite
8	Kp6	30 17 31.5	53 39 36.5	Siliceous rock
9	Kp22	30 18 23.9	53 39 56.6	Peridotite
10	Kp23	30 18 22.9	53 39 55.2	Peridotite
11	Kp24	30 18 23.1	53 39 54.9	Copper mineralization in the form of malachite and azurite
12	Kp25	30 18 23.1	53 39 54.9	Copper mineralization in the form of malachite and azurite
13	Kr1	29 59 6.8	54 03 39.6	Serpentinized peridotite
14	Kr2	29 59 6.7	54 03 39.5	Serpentinized peridotite
15	Kr3	29 59 7.1	54 03 40	Serpentinized peridotite
16	Kr6	29 59 7.3	54 03 38.7	Peridotite
17	Kr7	29 59 7.3	54 03 38.7	Laterite
18	Kr8	29 59 7.3	54 03 38.7	Limestone
19	Kr9	29 59 7.3	54 03 38.7	Limestone
20	Kr11	29 59 7.8	54 03 33.8	Limestone

Results

Color Composites

According to the spectral reflectance curves (Figures 6 and 7), the bands have higher reflectance than other bands to make the color combination of peridotite and serpentinite. In order to build the best color composites, at first spectral reflectance curves were plotted using ground control points (Figs. 6 and 7). Spectral reflection diagrams were compared with peridotite and serpentinite diagrams in the ENVI software archive, and the band reflection intensities had the highest reflection intensities

in bands 2 and 3, respectively (Figures 8 and 9). The bands that have the most reflection were used to make color combinations. Bands 2, 3, and 5 have the highest reflection intensity in the Landsat 8 image. The following equation is correct: $b_2 > b_3 > b_5 > b_6 > b_1 > b_4$. Therefore, RGB=532 will create the best contrast for peridotite units.

Data Fusion

The aim of remote sensing image fusion techniques is to integrate the information conveyed by data obtained

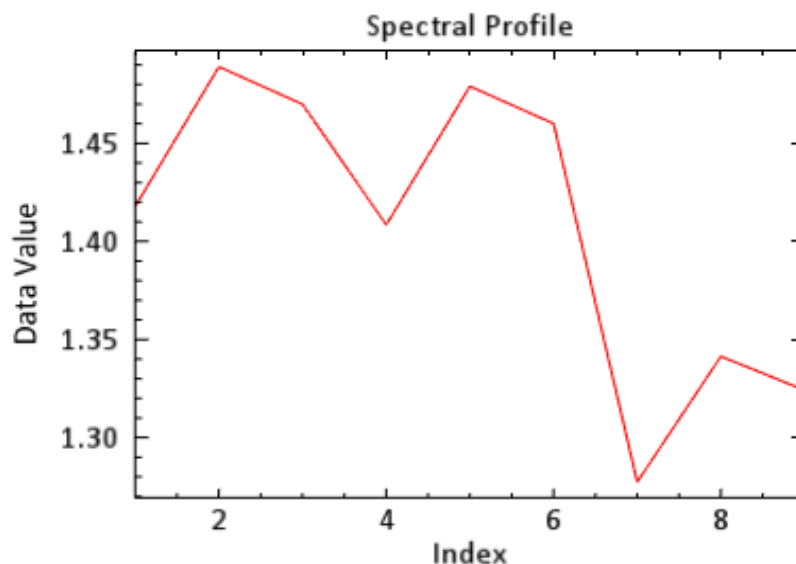


Figure 6. Spectral reflection diagrams of peridotites.

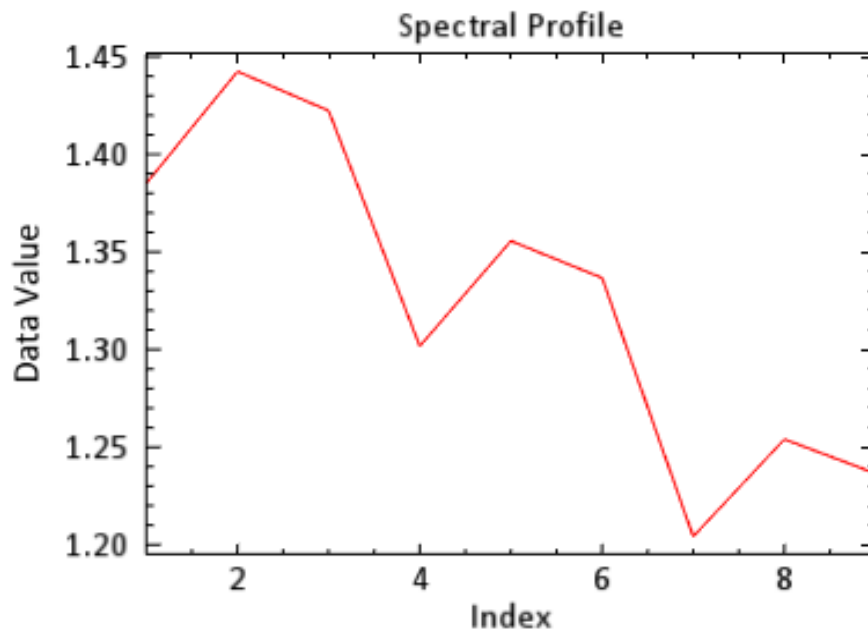


Figure 7. Spectral reflection diagram of serpentinized peridotite.

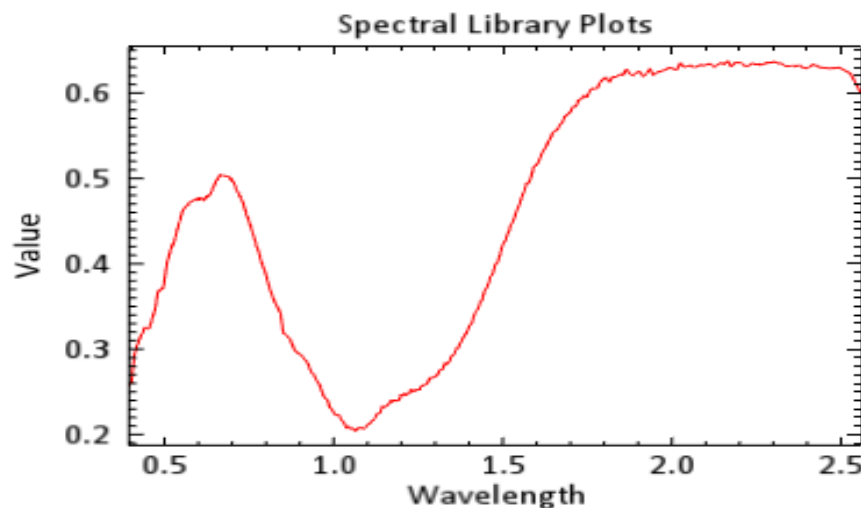


Figure 8. Spectral archive diagrams of peridotite.

with different spatial and spectral resolutions from satellites or aerial platforms in order to obtain higher quality images. The Gram-Schmidt Pan-Sharpener method was used to combine Pan images (15 m pixel size) with seven multispectral images (30 m pixel size) to produce a single 15 m pixel size [22]. The Gram-Schmidt Pan-sharpening method is more accurate than the Principal Component (PC) and Hue Saturation Value (HSV) methods because it uses the spectral response function of a given sensor to estimate the appearance of panchromatic data. Gram Schmidt Pan-Sharpener method is highly recommended for most applications.

Comparing the Z Profile of the original image with the Gram-Schmidt Pan-Sharpener image showed no difference in spectral information [23]. The result of this technique is entirely satisfactory, and the peridotite unit was well enhanced and detected using Landsat 8 fused data (Figure 10). Also, Figure 11 shows no fused image of Landsat 8.

Band Ratios

Band ratios are one of the important methods for rock unit's enhancement. Bands with the highest and lowest reflection were identified by spectral reflectance curves

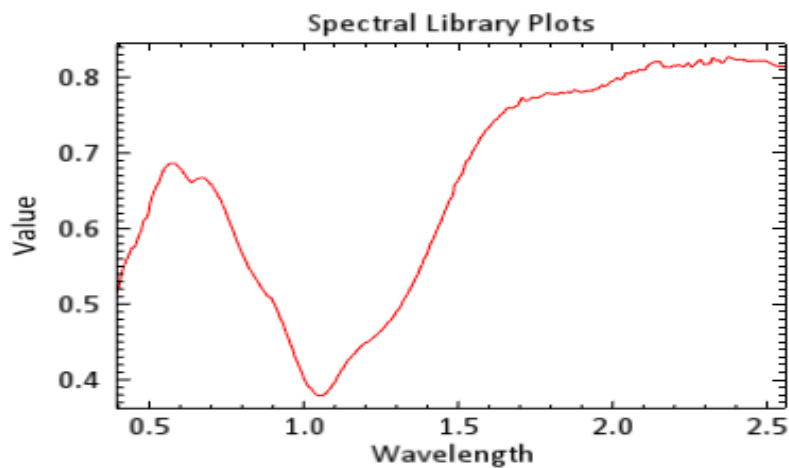
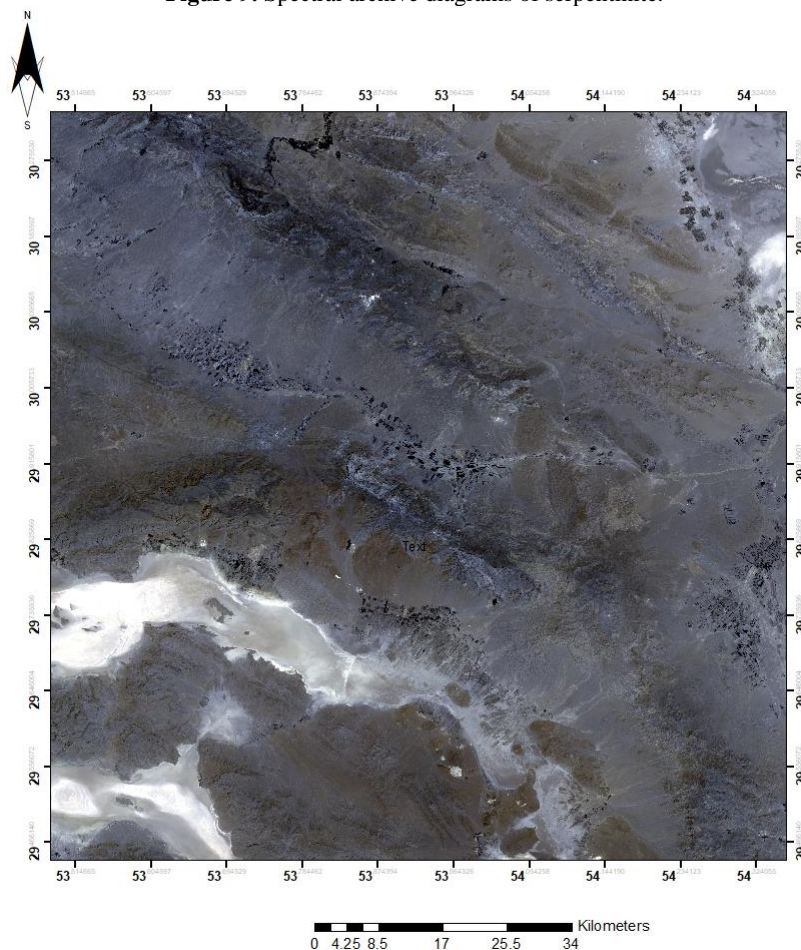


Figure 9. Spectral archive diagrams of serpentinite.



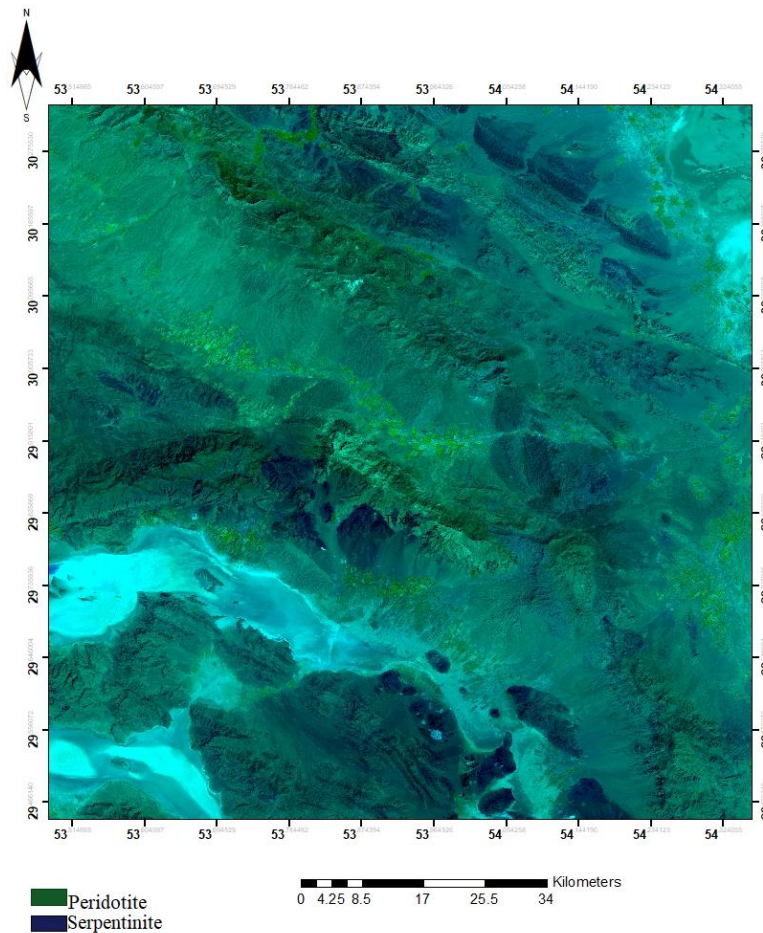


Figure 11. Fused image of Landsat 8.

and b7 the lowest reflection intensity:

$$RGB=(b2/b1), (b5/b1), (b6/b7)$$

Accordingly, the band ratio images of Landsat 8 were created and revealed that the below color composite has the best contrast for the peridotite and serpentinite:

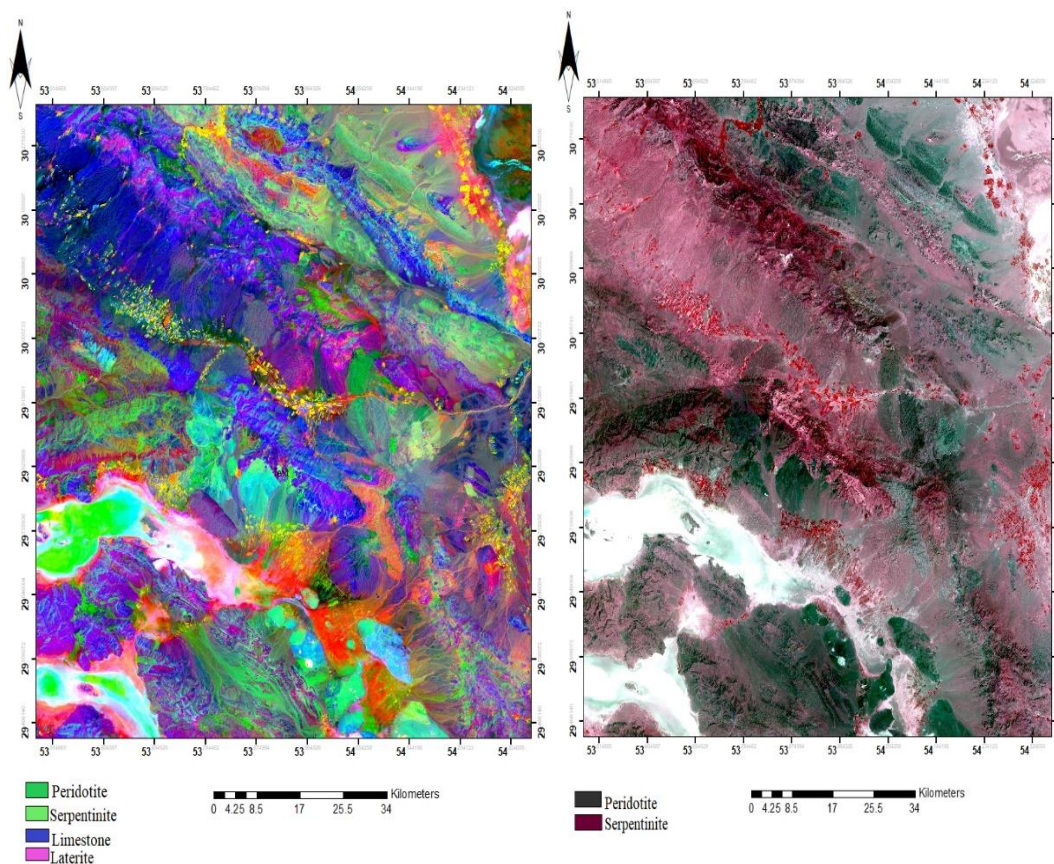
$$RGB=(b2/b1), (b5/b1), (b6/b7)$$

In the above color composite, the peridotite unit is blue, the serpentinite unit is light brown, and both are easily identified and differentiated (Figure 12).

Principal Component Analysis (PCA)

Principal Component Analysis is a powerful statistical technique that can compress the image and eliminate the unwanted effects of PCA [3]. Principal component analysis is a mathematical formula used to reduce the dimensionality of data. Therefore, the PCA technique allows the identification of standards in the

data and their expression in such a way as to emphasize their similarities and differences. PCA is a statistical and mathematical method with many applications for representing differences between satellite images. The most important uses of the PCA method in RS are concentrating and limiting information in a few specified channels and increasing the amount of information in these channels. Also, Principal Component Analysis (PCA) is a technique that transforms high-dimensional data into lower dimensions while preserving as much information as possible. The principal component analysis is done in both standard and selective methods. In the standard method, all bands are used to detect rock units; in the selected method, only high reflection bands are used. Two selective and standard methods were used in detecting rock units (Figure 13). The standard method



Figures 13. PCA technique for Landsat 8 data in standard and selective methods.



Figure. 12. Band ratio image RGB = (b2/b1), (b5/b1), (b6/b7) for Landsat 8.

had better results in detecting and slicing the studied rock units. The PCA method shows that RGB=PC6, PC2, and PC5 for Landsat 8 data have the best contrast for enhancing and detecting peridotite and serpentinite units. As a result, peridotite and serpentinite units are seen in dark green and light green colors, respectively.

Supervised Classification

The main advantage of supervised classification is that it allows you to collect data or generate data output from previous experience. Supervised classification strongly depends on training locations, the skill of the individual processing the image, and spectral discrimination of classes. The separation of similar spectral assemblies and their class division with the same

spectral behavior is called satellite information classification. In other words, classifying the pixels that make up an image, assigning each pixel to a particular class, is called satellite information classification. In this study, the images of Landsat 8 have been used for supervised classification by SAM, SID, and SVM methods. The Spectral Angle Mapper (SAM) and Spectral Information Divergence (SID) methods perform based on the spectral reflectance curve for one special pixel. Among the mentioned methods, the SID method has better results for slicing and detecting the studied rock units. In this operation, the training points are defined for six classes, including peridotite, serpentinite, and laterite units, in relation to the other three defined classes. In the final classification image, the peridotite

and serpentinite units are seen in red and yellow, respectively, and are well detectable and separable from surrounding units (Figure 14).

Validation

In order to control the supervised classification operation of SID, some control points were considered for the accuracy and evaluation of this method. Twenty auxiliary points (Table 2) were marked on the supervised map, and the nineteen points showed the position of the studied rock units correctly. Thus, SID classification should be 90% accurate using this method (Figure 15).

Discussion

The current study aimed to enhance, detect, and slice peridotite and serpentinite units from adjacent units. It confirmed that combining field and remote sensing data can have trustful results for identifying and separating these units. During field studies, 40 points of peridotite, serpentinite, lateritic, and calcareous units were reviewed, and GPS recorded their positions.

The use of data fusion techniques, fortunately, was effective. These techniques created a high enhancement for peridotite and serpentinite units from other units. Also, based on the current study, the Gram-Schmidt method has had more efficiency than other methods for enhancing peridotite and serpentinite units. Different techniques, such as band ratio and PCA methods, have improved and brought more enhancement and detection for peridotite and serpentinite units.

RGB=(b2/b1), (b5/b1), (b6/b7)

In the band ratio method, color composite with RGB=(b2/b1), (b5/b1), and (b3/b7) has the best contrast for peridotite and serpentinite units. Also, the PCA methods by the standard method RGB=PC6, PC2, and PC5 with the best contrast have led to better detection and slicing of the studied units. Various methods of supervised classification have been applied. The result of all of these studies illustrated that among the SAM, SID, and SVM methods, Spectral Information Divergence (SID) has the best performance in the detection and slicing of peridotite and serpentinite units. Due to the

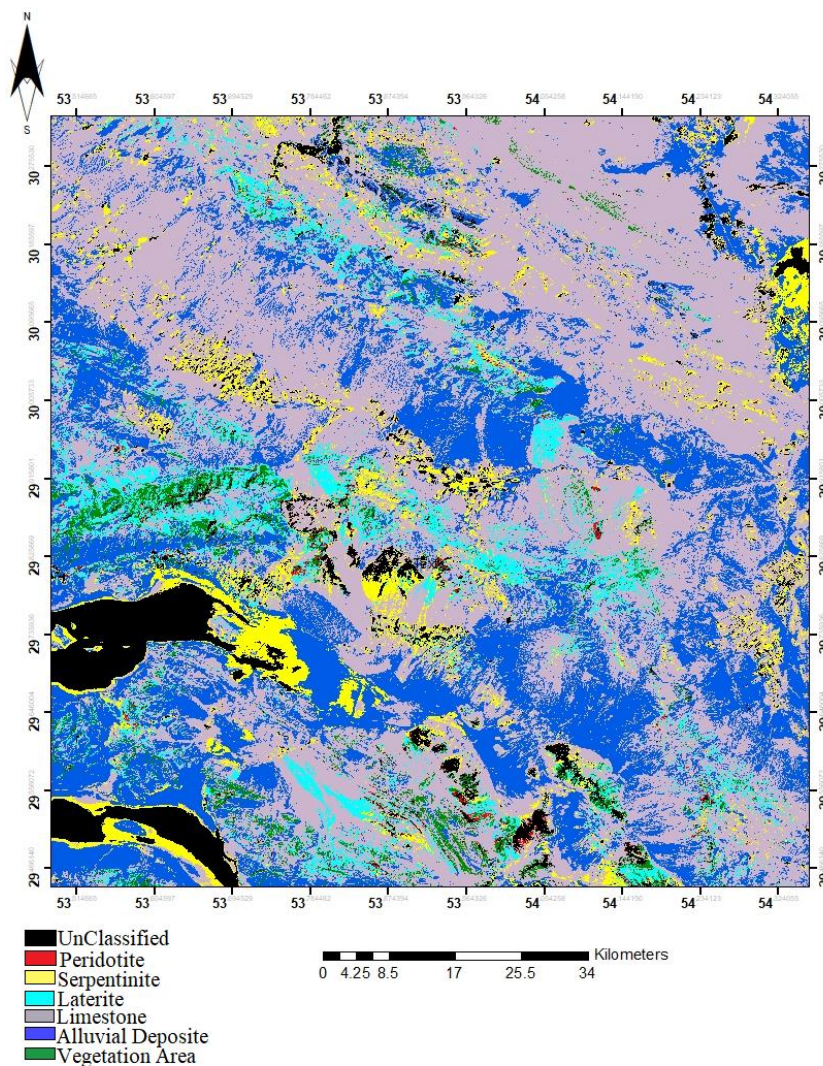


Figure 14. Supervised classification image for Landsat 8. In this image, the peridotite unit is red, the serpentinite unit is yellow, and both units contrast perfectly with other units. This image can be the basis for the preparation of geological maps of this area, especially for the enhancement and detection of the peridotite unit of Bavanat.

separation of similar spectral sets and the classification of pixels that have the same spectral behavior, the classification was completed using the SID method. In this classification, the detection and slicing of peridotite and serpentinite units were well achieved by assigning each pixel to a specific class. Finally, after performing classification, the validation operation was performed, and the SID classification detected rock units with 90% accuracy. Therefore, this supervised classification method is recommended for other areas with similar conditions. The classification image created in these studies can be used as a basic geological map in the exploration studies for peridotite and serpentinite units.

Conclusions

This study proved that based on the combination of field and remote sensing data, valuable information could be obtained on how to expand the target rock units and the method of separating them from other units. The use of new methods and new technologies along with the use of traditional exploration methods can lead to valuable results. Based on the results of this study the methods of principal component analysis and supervised classification of SID and finally the validation and evaluation operations (Fig. 15) have the correct results in relation to the detection and slicing of peridotite and

Table 2. Ground control points.

Row	Sample Number	Y	X	Description
1	Kp1	30 16 09	53 40 33.5	Red laterite
2	Kp7	30 17 31.3	53 39 36.2	Serpentinized peridotite
3	Kp8	30 17 31.3	53 39 35.3	Serpentinized peridotite
4	Kp9	30 17 29	53 39 33.4	Red laterite
5	Kp10	30 17 32.9	53 39 37	Peridotite
6	Kp12	30 17 9.8	53 40 54.2	Serpentinized peridotite
7	Kp14	30 17 8.6	53 40 54.8	Serpentinized peridotite
8	Kp15	30 17 6.2	53 41 5.9	Red laterite
9	Kp16	30 16 58.2	53 41 14.7	Red laterite
10	Kp17	30 18 31.2	53 40 1.2	Peridotite
11	Kp18	30 18 33	53 40 02	Peridotite
12	Kp19	30 18 32.9	53 40 1.7	Serpentinized peridotite
13	Kp20	30 18 33.4	53 40 1.9	Peridotite
14	Kp21	30 18 24.4	53 39 57	Serpentinized peridotite
15	Kr4	29 59 8.1	54 03 42.3	Red laterite
16	Kr5	29 59 6.8	54 03 39.1	Serpentinized peridotite
17	Kr10	29 59 6.7	54 03 36.3	Peridotite
18	Kr13	29 59 6.7	54 03 39.1	Peridotite
19	Kr14	29 59 6.5	54 03 38.6	Peridotite
20	Kr15	29 59 6.2	54 03 38.8	Peridotite

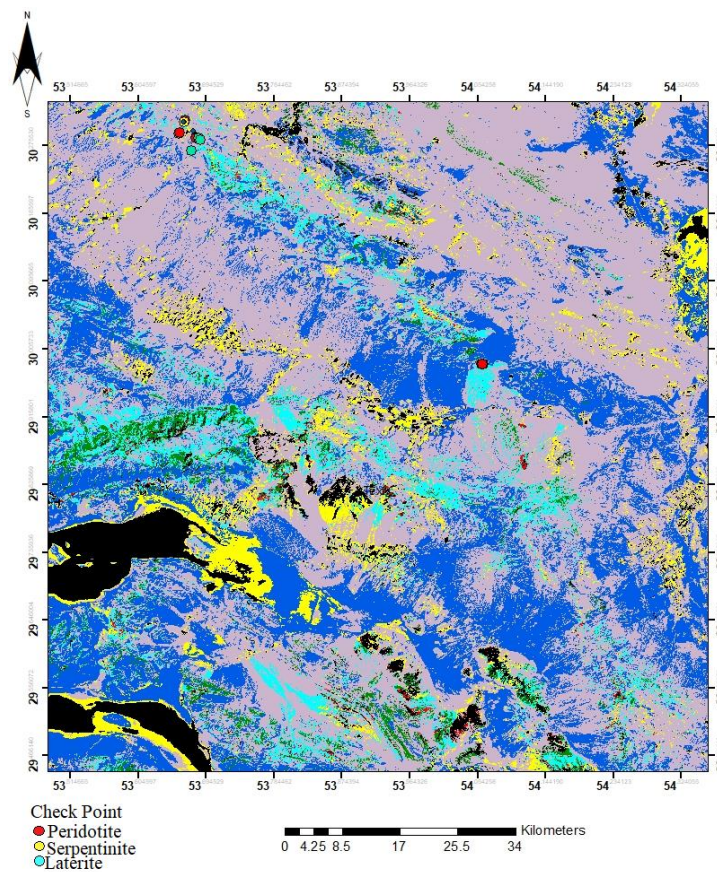


Figure 15. Validation (Check Point).

serpentinite units. These results can be used in similar areas.

Acknowledgement

Special thanks to Mr. Zare for his efforts in holding the field. Constructive reviews especially by Dr. I. Monsef (Institute for Advanced Studies in Basic Sciences (IASBS), Zanjan) are warmly acknowledged.

References

- Oveisi B. Geological map of Surian. Scale 1:100,000. Geological Survey of Iran, 2001.
- Safaei H, Sharifi M, Tabatabaieimanesh SM, Chopannejad R. Separation of lithology units and shear zones of the northern Golpayegan metamorphic complex using digital satellite data processing. Conference on Applied petrology, 2010.
- Alavipanah SK. Application of remote sensing in Earth sciences (Soil science), Tehran University Press. 2003;478p. (in Persian)
- Gupta R. P. Remote sensing geology. second edition, springer - verlag, Berline, 2003; 655p.
- Taherzadeh L, Noori Khankahdani K, Amiri A, Nikeghbal N. Detection and slicing of Neyriz Tang-e-Hana marbles and skarns based on remote sensing data. The second Conference of Applied Petrology Islamic Azad University Khorasgan Branch. 2010.
- Sekhavati A, Amiri A, Ranjbar H, Noori Khankahdani K. Compared the results of the processing of Aster images and ETM for detection of Pb and Zn ore lithological units Bahabad area - Yazd, the second Congress of economic geology of Iran. 2011.
- Faridi R, Yaghpour A, Hezareh MR, Masudi F. Remote sensing studies for the detection of lineaments and alteration zones (North West of Robat Khan). The 30th meeting of Earth Sciences, Geological Survey of Iran, Tehran, Iran, 2011.
- Gomez C, Delacourt C, Allemand P, Ledru P, Wackerle R. Using ASTER remote sensing data set for geological mapping, in Namibia. *Phy. Chem. Earth, Parts A/B/C*, 2005; 30(1-3): 97-108.
- Nikolakopoulos KG, Tsombos PI, Photiades A, Psonis K. Using remote sensing multispectral data and GIS techniques for the geological mapping of Halki Island. *Bull. Geol. Soc. Greece*, 2016; 47(3): 1500-1509.
- Lillesand TM, Kiefer RW. Remote Sensing and Image Interpretation (4th end). New York, John Wiley and Sons, 2000.
- Charou E, Stefouli M, Dimitrakopoulos D, Vasiliou E, Mavrantza O.D. Using Remote Sensing to assess the impact of mining activities on land and water resources. *Min. Water Env*, 2010; 29: 45-52.
- Ruisi Z, Min C, Jianping C. Study on geological structural interpretation based on Worldview-2 Remote Sensing image and its implementation. *Procedia Env. Sci.* 2011; 10: 653 – 659.
- Noori Khankahdani K, Zarei E. Comparison between standard and selective PCA methods in the enhancement and detection of the dunite of Neyriz ophiolite sequence. 16th Annual Conference, Geological Society of Iran, Shiraz University, 2012.
- Shahvaran S. Investigation of economic potential of ultramafic laterites east of Kooapan and Rostami villages (northeast of Fars province). 2012.
- Khademi A. Investigation of mineral potential of nickel laterite south of Ghaderabad, Fars province. 2010.
- Ghasemi N, Asadi Harouni H, Darvishzadeh A, Vosoughi Abedini M. Application of remote sensing to determine the potentials of nickel-bearing laterites in Sarchahan. 30th Earth Sciences Conference, Tehran, Geological Survey of Iran, 2012.
- Monsef I, Monsef R, Mata J, Zhang Z, Pirouz M, Rezaeian M, Esmaili R, Xiao W. Evidence for an early-MORB to fore-arc evolution within the Zagros suture zone: Constraints from zircon U-Pb geochronology and geochemistry of the Neyriz ophiolite (South Iran). *Gondwana Research*, 2018; 62: 287-305.
- Ricou L.E. Evolution structurale des Zagrides. La region Clef de Neyriz (Zagros Iranien). *Mem. Soc. Geol. Fr., Nouvelle Serie-Tom LV*, 1976; 55(125), 140 p.
- Arvin M. Petrology and geochemistry of ophiolites and associated rocks from the Zagros suture, Neyriz, Iran. Ph.D. thesis, London University, London, England, 1982.
- Hoshmandzade A, Sohili M. Description of Geological Map of Eqlid Sheet, Geological map of Iran. 1:250000 Series sheet G10, Geological survey of Iran, 1990.
- Zurmand M, Noori Khankahdani K, Ghadami Gh, Masoodi M. The Use of Remote Sensing Techniques for Enhancement and Detection of Kooapan Laterites (Zagros Region), North East of Shiraz. *J. Adv. Biores*, 2015; 5:104-110.
- Laben CA, Brower BV. Process for Enhancing the Spatial Resolution of Multispectral Imagery using Pan-Sharpning. U.S. Patent, 2000; 6, 011, 875.
- Amer A, El Mezayen A, Hasanein M. ASTER spectral analysis for alteration minerals associated with gold mineralization. *Ore Geol. Rev.* 2016; 75: 239-251.
- Faust NL. Image enhancement. In: Kent, A. Williams, J.G. (Eds.) Supplement 5 of Encyclopedia of Computer Science and Technology. 20: Marcel Dekker, Inc., New York, 1989.